Vol. 707: 15–29, 2023
https://doi.org/10.3354/meps14261

MARINE ECOLOGY PROGRESS SERIES
Mar Ecol Prog Ser

Published March 9

# Impacts of thermal effluent on *Posidonia oceanica* and associated macrofauna

**Andrew Agius[1,*,#], Luka Seamus Wright[2,#], Joseph A. Borg[1,#]**

[1]Department of Biology, University of Malta, Msida, MSD 2080, Malta
[2]Oceans Institute, University of Western Australia, Perth, WA 6009, Australia

ABSTRACT: *Posidonia oceanica* is a dominant marine macrophyte in shallow coastal waters of the Mediterranean and arguably the most important habitat-forming species. While the effects of elevated seawater temperature on *P. oceanica* have been studied in laboratory experiments and observed in the field following marine heatwaves, it appears that no field surveys to assess long-term influence are available. Making use of the exponential temperature gradient ($k$ = 0.05 $m^{-1}$) created by thermal effluent from a fossil fuel power station that has been operating for 3 decades, we aimed to fill this knowledge gap by assessing the *in situ* effects of elevated temperature (ΔT = 0.39°C) on *P. oceanica* and associated motile macrofauna. Seagrass leaf area and biomass alongside epiphyte biomass rapidly decreased on moving towards the thermal outflow, but no such change was evident for leaf number and shoot density. The observed differences in seagrass shoot attributes may result from differential adaptation of various parts of the plant to thermal stress. Macrofaunal species richness increased on moving towards the effluent source but evenness decreased. These results predict a near-future scenario where even small rises in seawater temperature in the coming decades will impact some attributes of *P. oceanica* and its epiphytes and cause a shift in the community composition of associated macrofauna towards fewer dominant species.

KEY WORDS: Climate change · Sea warming · Thermal pollution · Natural experiment · Seagrass meadows · Community ecology



## 1. INTRODUCTION

In the Mediterranean, the endemic seagrass *Posidonia oceanica* serves as a highly important ecosystem engineer that forms extensive meadows down to depths of around 40 m, which are arguably the most important habitat type in the shallow coastal waters of the region (Boudouresque et al. 2012). Unfortunately, various anthropogenic stressors and climate change are causing a global decline of seagrasses (Orth et al. 2006, Waycott et al. 2009, Telesca et al. 2015, Thomson et al. 2015) including *P. oceanica* (Marbà et al. 1996, Bianchi & Morri 2000, Burgos et al. 2017). *P. oceanica* habitat has declined by an estimated ~34% in the past 50 yr (Telesca et al. 2015), which may be outpacing the global rate of seagrass decline (Marbà et al. 2005). Worst-case scenarios predict that this seagrass could become functionally extinct by 2100 (Chefaoui et al. 2018), although it appears that the rate of decline of *P. oceanica* and other species of seagrass has abated in recent years and in some areas *P. oceanica* cover has increased or remained unchanged (González-Correa et al. 2007, de los Santos et al. 2016).

Loss of *P. oceanica meadows* is concerning because they comprise one of the most productive ecosystems on earth (Boudouresque et al. 2012), underpinning complex food webs that support highly diverse biotic assemblages and provide other valuable ecosystem goods and services (Burgos et al. 2017). *P. oceanica* meadows are consequently listed as priority natural habitat in European Union (EU)

*Corresponding author: agiuza@gmail.com
#All authors contributed equally to this study

member states, for which special management and conservation plans must be implemented (EEC 1992). The seagrass is also important within the context of monitoring the ecological status of coastal waters under the EU's Water Framework Directive, since it is one of 4 'Biological Quality Elements' that are indicated for monitoring in the Directive.

Sea temperature has been recognised as a main factor determining seagrass production and health, including for *P. oceanica* (Zupo et al. 1997, Pagès et al. 2018). Deviation from the optimal temperature range of marine macrophytes may lead to adverse impacts on habitat and associated biota (O'Connor 2009, Thomson et al. 2015). *P. oceanica* survives in the broad temperature range of 9–29°C, but its optimal growth occurs within the range 15–18°C (e.g. Lee et al. 2007, Pagès et al. 2018), while temperatures in excess of 29°C are deemed detrimental to the plant (Boudouresque et al. 2012). Shoot mortality and adverse physiological effects occur at a seawater temperature of 27°C and above, if such elevated temperatures persist over a period of several weeks or longer (Marbà & Duarte 2010). Sexual reproduction is triggered at a temperature of ~20°C (Boudouresque et al. 2012), but when temperature exceeds 27°C, the growth of young plants is limited through inhibition of their photosynthetic capacity (Guerrero-Meseguer et al. 2017)

Global climate change will result in ocean warming (Huang et al. 2015), such that the average sea surface temperature could potentially increase by 3.7°C by the year 2100, as predicted by Representative Concentration Pathway (RCP) 8.5, a general circulation model assuming very high greenhouse gas emissions. A model assuming stringent mitigation measures and curbing of greenhouse gas emissions could on the other hand result in a mean increase of just 1°C (IPCC 2014). Therefore, the prediction is that the mean sea surface temperature should rise by at least 1°C by 2100, while warming of the Mediterranean Sea is occurring at a faster rate than the global average (Jordà et al. 2012). Given that increased sea temperature poses a potential threat to *P. oceanica*, it is crucial to gain an understanding of the effects of sea warming on seagrass and the habitat it forms, since this will help to better predict potential adverse effects.

Several studies have addressed the influence of elevated temperature on *P. oceanica*, but these were either conducted following heatwaves in Mediterranean coastal areas (e.g. Marbà & Duarte 2010, Helber et al. 2021) or entailed laboratory experiments designed to assess the response of seagrass to increased water temperature (Marín-Guirao et al. 2016, 2017, 2018, Guerrero-Meseguer et al. 2017, Hernán et al. 2017, Beca-Carretero et al. 2018, Pagès et al. 2018, Ruiz et al. 2018) or to a combination of elevated temperature and other environmental stressors such as burial and overgrazing (Guerrero-Meseguer et al. 2020), nutrient overloading (Helber et al. 2021) and increased ammonium levels (Ontoria et al. 2019). Research aiming to understand the *in situ* long-term effects of elevated sea temperature on *P. oceanica* meadows and associated biota are lacking. Such insights from natural experimentation would be valuable in contributing to our understanding of seagrass thermal tolerance and plasticity and predicting the effects of ocean warming on the seagrass ecosystem.

Within the context of investigating the influence of sea warming on seagrasses and seagrass habitats, coastal sites that are subjected to natural or human-induced thermal alterations may serve as a natural *in situ* laboratory, since they can be used to assess the impacts of elevated sea temperature on marine species and habitats. Sites where thermal effluents are introduced to the marine environment have long been used in this regard (Thorhaug et al. 1978, Langford 1990, Schiel et al. 2004). The influence of power station effluent on benthic assemblages and species including *P. oceanica* has been assessed in the Mediterranean, but without specifically reporting effects of elevated sea temperature on the studied biota (Matteucci et al. 2011). In Malta, the inlet known as Il-Ħofra ż-Żgħira (HZ), located on the southeastern coast, receives thermal effluent from the turbine cooling system of the Delimara Power Station (DPS), which is the main power-generating fossil fuel station in the Maltese Islands (see Fig. 1). At HZ, the thermal effluent is released at a temperature of around 8°C above ambient in the inner parts of the inlet. This implies that the ambient sea temperature in the immediate vicinity of the discharge outlet in HZ can increase from 27°C to 35°C in summer and from 16°C to 24°C in winter. Mixing of the effluent with the sea results in a gradient of decreasing water temperature between the discharge point and the mouth of the inlet, giving the site particular physical characteristics in terms of elevated seawater temperature, which is expected to have an appreciable influence on the marine habitats and species present there (see Fig. 2).

Using space for time substitution, the present study generally aims to establish whether the thermal effluent discharged at HZ is affecting *P. oceanica* and associated motile macroinvertebrate assemblages. Some effects are presumed given the adverse influ-

ence of elevated sea temperature on the biology of the seagrass and ultimately on meadow structure, which is expected to influence the associated macrofaunal communities. Specifically, we utilise this temperature gradient as a proxy for near future climate scenarios in the coming 2 decades to shed light on the effect of elevated seawater temperature expected around Malta on *P. oceanica* at the plant and habitat levels. To address this aim, *P. oceanica* and associated motile invertebrate fauna were sampled at HZ and at Il-Ħofra l-Kbira (HK), 2 inlets that are adjacent to each other and have similar environmental characteristics, but the latter is not under the influence of thermal effluent (see Fig. 1). After empirically determining the robustness of the natural temperature treatment provided by the thermal effluent, we tested the null hypotheses that temperature has no effect on *P. oceanica* leaf density, leaf area, leaf biomass, specific leaf area (SLA) as an indicator of tissue density, shoot density as well as macrofaunal abundance, richness, diversity and evenness. In addition to testing for changes in these variables along the thermal gradient at HZ, we compared the magnitude of change to that observed at the control site in order to account for potential confounders associated with distance from shore, such as depth.

## 2. MATERIALS AND METHODS

### 2.1. Study sites and pilot survey

The 2 sites considered in the present study are located adjacent to each other but separated by a peninsula known as Ras il-Fniek (Fig. 1). The 2 inlets have very similar environmental characteristics, including bathymetry, geology and exposure. Both inlets lack any riverine inputs and have identical salinity (see Section 3.1). Water depth is <0.5 m adjacent to the shore and ~15 m at the mouth of both HZ and HK.

Thermal effluent originating from the turbine cooling system of the natural gas-fired DPS is released within HZ through a single discharge outlet located at sea level at the inner eastern part of the inlet. The type of cooling system used at the DPS is of the 'once through' type, wherein seawater is taken up from within Marsaxlokk Bay (located southwest of HZ), passed through the power station, and eventually discharged to the sea at HZ via an underground pipeline. The cooling system has been in operation since commissioning of the DPS in the early 1990s. Through the 1990s and early 2000s, the DPS was upgraded several times, and in 2014, the heavy fuel oil-fired power station was converted to use liquified natural gas to fire its turbines.

Baseline information on the occurrence and distribution of *Posidonia oceanica* meadows and other benthic habitat types present in the 2 study sites, HZ and HK, was obtained by undertaking a pilot survey. During the pilot survey, conducted in June 2016, 5 transects, each having a length of 100 m on the seabed, were surveyed at each site using SCUBA diving. At HZ, the starting point of each transect was the thermal discharge point (Fig. 1). At HK, the starting point of each transect was taken to be location of a hypothetical discharge point when a map of HZ is superimposed on that of HK (Fig. 1). During the survey, the divers noted the occurrence and distribution of *P. oceanica* meadows and other habitat types — photophilic algae on hard substrata, bare sand habitat and seagrass *Cymodocea nodosa* meadows — along each of the 5 transects. The findings from the pilot study confirmed the occurrence of extensive *P. oceanica* meadows at both sites, starting at 10–15 m from shore at HK and ~20 m from shore at HZ. On considering the distribution of *P. oceanica* in the 2 study inlets, 4 plots to sample the seagrass were chosen in each of the 2 study sites. The sampling plots were located such that there was a continuous seagrass cover throughout the sampling area, since seagrass cover at both inlets was fragmented, with various sand channels and patches. The depth of the water column varied between 3 and 5 m at all plots in both bays.

### 2.2. Temperature gradient

The main water quality parameters considered were temperature and pH, for which data were collected *in situ* at intervals of 2 m along each of the five 100 m transects at HZ and HK (Fig. 1), using a Hanna HI 9828 Multiparameter meter. Measurements were taken by A. Agius at the sea surface on 7$^{th}$ September 2016 and 8$^{th}$ February 2017, close to the yearly maximum and minimum seawater temperature respectively. Upon revisiting HZ on 20$^{th}$ April and 4$^{th}$ June 2021, L. S. Wright noted that, within the seagrass meadow, temperature dropped by 4.5°C between 0 and 51 m from the effluent source (corresponding to 1.8 and 3.8 m depth) and then only dropped a further 1°C at 95 m distance (5 m depth). This strongly suggested the presence of a thermocline caused by the extreme temperature difference between the overlying effluent and underlying bay water and an exponential temperature trend in the seagrass meadow.

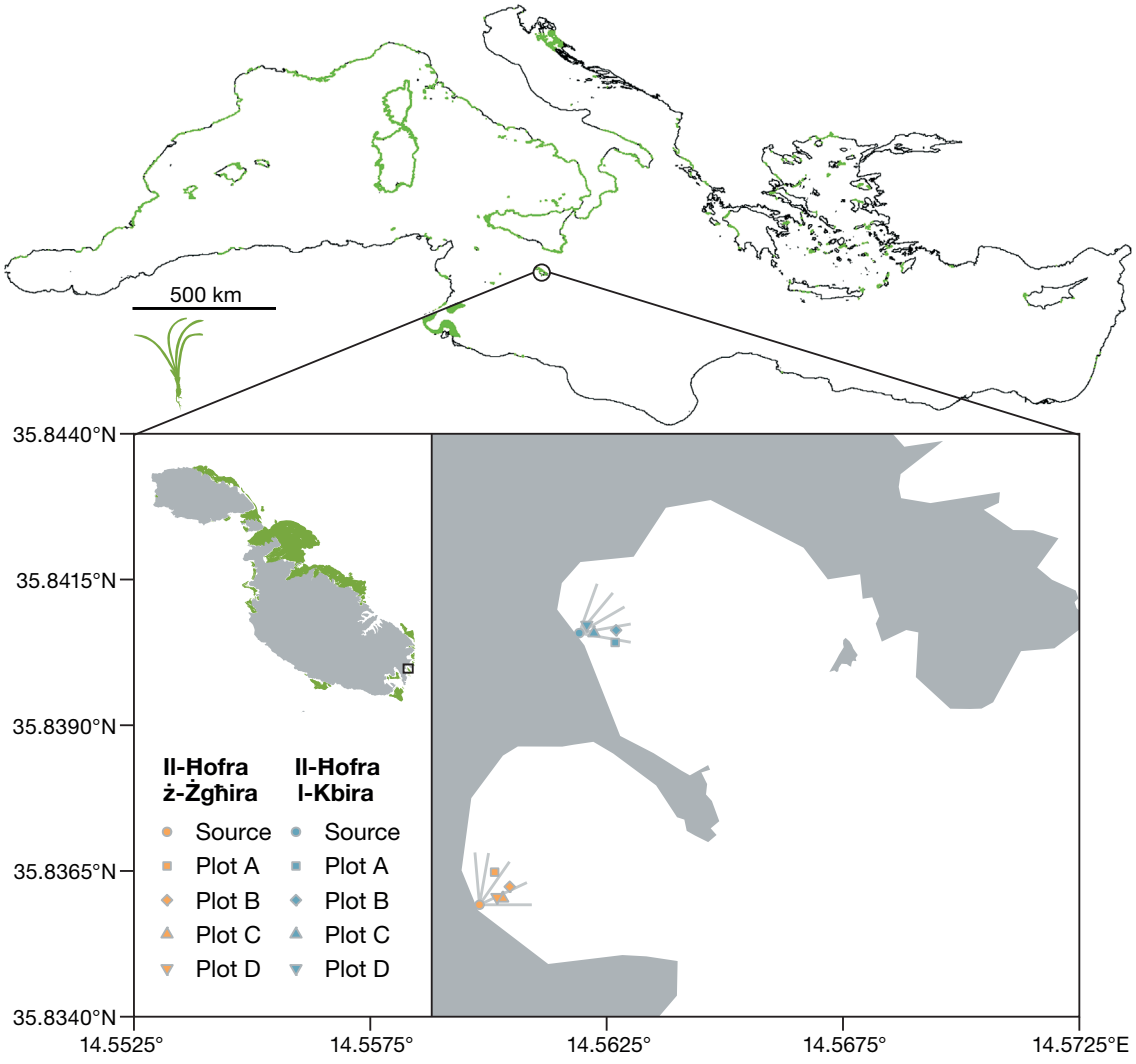


Fig. 1. Location of the 2 study sites and 4 plots within each site on the southeast coast of Malta (inset) in the seagrass-rich central Mediterranean. Green areas are *Posidonia oceanica* meadows. Grey lines represent the five 100 m transects surveyed at each of the 2 study sites. Plots A to D are located along the thermal gradient at Il-Ħofra ż-Żgħira. At Il-Ħofra l-Kbira, the study design was replicated to control for any effects that were unrelated to the thermal effluent. Maps are oriented north in the WGS 84 coordinate reference system and rendered according to the equirectangular projection. Shapefiles for land masses and seagrass meadows were sourced from https://osmdata.openstreetmap.de and https://data.unep-wcmc.org respectively

To achieve higher resolution and be able to fit an exponential model, A. Agius returned to HZ and HK on 7th June 2022 to repeat the 2016/17 temperature and pH measurements in the seagrass meadow.

### 2.3. *Posidonia oceanica*

Seagrass plots were marked at distances of 36.35–68.63 m from the effluent source at HZ and 21.22–70.53 m from the shore at HK (Fig. 1). To obtain estimates of *P. oceanica* shoot density, 3 counts for this attribute were made at each plot using a 35 × 35 cm quadrat. Ten shoots of *P. oceanica* were then collected from each plot for morphometric studies. All samples were collected on the 7th and 8th December 2016. In the laboratory, each seagrass shoot was separated into the individual leaves, characterised as adult, intermediate or juvenile (Giraud 1979), and the length and width of each leaf measured to the nearest 0.5 mm. Leaf area was subsequently estimated as length × width. The leaves were then scraped to remove epiphytes, which were collected in pre-weighed containers. The leaf epiphytes mainly comprised encrusting algae, including *Melobesia* sp., short filamentous algae, hydroids and serpulid

polychaetes. Leaves and epiphytes were left to airdry and afterwards oven-dried at 70°C for 14 h before measuring their dry biomass to the nearest 0.1 mg. SLA was calculated as leaf area divided by leaf biomass for each leaf as well as at the shoot level. SLA is a common metric in seagrass ecology (de los Santos et al. 2012) and is the inverse of leaf mass per area (LMA) and negatively related to tissue density, toughness and longevity (de los Santos et al. 2016).

### 2.4. Macrofauna

Motile macrofauna associated with *P. oceanica* meadows were sampled on 7$^{th}$ and 8$^{th}$ December 2016 using SCUBA diving and the hand net method (Russo et al. 1985), whose appropriateness and efficiency to sample the fauna associated with the leaf stratum of the seagrass has been shown in previous studies (e.g. Mazzella et al. 1989, Gambi et al. 1992, 1998). The net opening measured 0.4 × 0.2 m and had a 0.5 mm mesh. Two hand net trawls were made at each plot, centred around the sampling points indicated in Fig. 1. A fibreglass tape was laid out in a zig-zag pattern, overlaid on the respective sampling station by one of the divers and the other diver followed the tape for a distance of 60 m with the net, such that the total area sampled per trawl was 24 m$^2$. The faunal samples were taken to the lab and preserved in 5% formaldehyde in seawater until identification to the lowest possible taxon.

### 2.5. Data analysis and visualisation

Data analysis was performed using R v4.0.2 (R Core Team 2020) within the integrated development environment RStudio v1.3.1093 (RStudio Team 2020). All response variables were tested against the continuous explanatory variable distance from shore and the categorical explanatory variable site with the 2 levels HK and HZ. In the case of detailed plant-level analysis, we added the factor growth stage with the 3 levels juvenile, intermediate and adult to our explanatory variables. (Generalised) linear models were sufficient in most cases, but June temperature and pH data at HZ were best described by exponential and polynomial models, fit with the *gnls* function of nlme v3.1-151 (Pinheiro et al. 2020) and the *lm* base function respectively.

Visual data exploration revealed outliers in SLA, which were removed prior to analysis, as well as right-skew in most linear response variables. Since transformation of response variables should generally be avoided (Zuur et al. 2009), gamma distributions were fitted to the data with the R package fitdistrplus v1.1-3 (Delignette-Muller & Dutang 2015). If the gamma distributions fit the univariate data better than Gaussian distributions, gamma generalised linear models with logarithmic link functions were built with the *glm* base function to improve normality of residuals. If this did not also improve homogeneity of variance, generalised least squares models, accounting for heterogeneity by assigning weights based on explanatory variables, were built with the *gls* function and *weights* argument of nlme v3.1-151 (Pinheiro et al. 2020).

Model fitting was performed using standard graphical techniques (plotting residual histograms, quantile–quantile plots and residuals vs. explanatory variables) and the Akaike information criterion (Zuur et al. 2009). Type II and III sums of squares tests were performed with the *Anova* function of car v3.0-10 (Fox & Weisberg 2019). Besides probability (p) values, *F* statistics are reported for simple linear models while chi-square ($\chi^2$) statistics are presented for generalised linear models and generalised least squares. *t* statistics (effect size divided by SE of the effect size) are provided for nonlinear models and pairwise contrasts between *P. oceanica* growth stages (the only factor with >2 levels).

Following identification of macrofauna, a species-abundance matrix was constructed and species richness, Shannon-Wiener diversity index (Shannon 1948) and Pielou's evenness index (Pielou 1966) were calculated. While the univariate data were analysed as described above, multivariate data (i.e. the entire species-abundance matrix) were analysed with PERMANOVA (Anderson 2001) after initial testing for homogeneity of dispersion (Anderson 2006). Additionally, similarity percentage analysis (Clarke 1993) was used to identify species responsible for between-group differences. Using Bray-Curtis distance matrices, these steps were implemented in the R package vegan v2.5-7 (Oksanen et al. 2020). All multivariate analyses were run with 9999 permutations. Results are reported using pseudo-*F* statistics and p-values.

Descriptive statistics were calculated using psych v2.0.12 (Revelle 2020), and then visualised using ggplot2 v3.3.3 (Wickham 2016) and cowplot v1.1.1 (Wilke 2020). Nonmetric multidimensional scaling (nMDS) points and ellipses were calculated in vegan and plotted in ggplot2 with the *veganCovEllipse* function (Oksanen et al. 2014). The map in Fig. 1 was plotted in QGIS 3.2 (https://qgis.org) and all figures

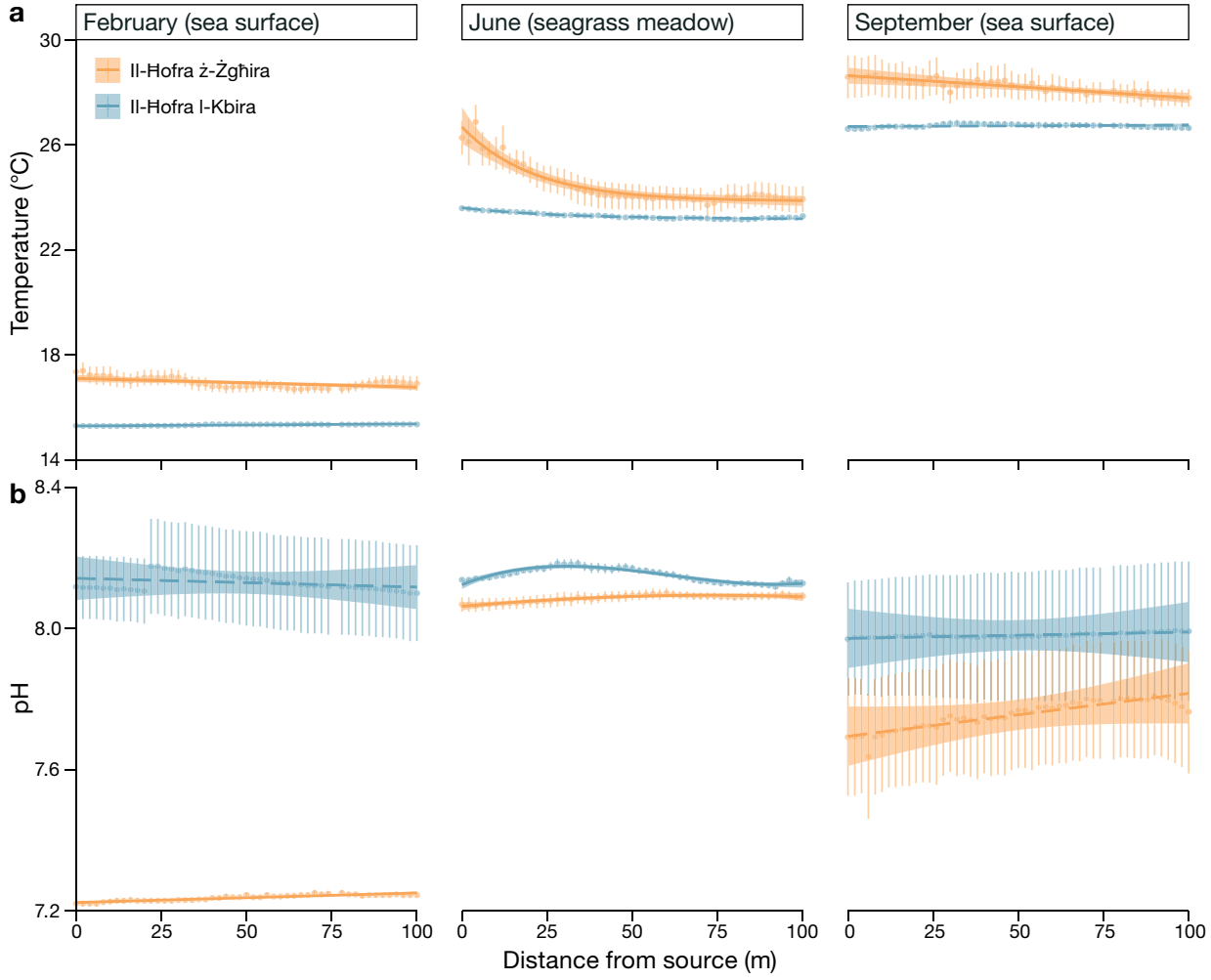


Fig. 2. Seawater (a) temperature and (b) pH in relation to distance from the effluent source at the elevated temperature site (Il-Ħofra ż-Żgħira) and from the coast at the reference site (Il-Ħofra l-Kbira) (see Section 2.2. for sampling dates). Note the presence of a thermocline created by the effluent at Il-Ħofra ż-Żgħira which causes temperature to drop exponentially in the *Posidonia oceanica* meadow between 0 and 5.4 m depth (June) in contrast to the linear trend at the sea surface (February and September). Point-ranges are means ± SEM (n = 5). Lines and ribbons are model predictions and 95% confidence intervals. Solid lines indicate a significant change with distance at the 95% confidence level, while dashed lines indicate no change

were edited in Affinity Designer (https://affinity.serif.com). R code, all data, and analytical details are available at https://github.com/lukaseamus/thermal-effluent.

## 3. RESULTS

### 3.1. Temperature gradient

Sea surface temperature (SST) across months is 2.02 ± 0.54°C (mean ± SEM, n = 10) higher at the point of thermal outflow than at an equivalent point at the reference site (Fig. 1). This difference is maximal in February, when SST at the effluent source is 2.05 ± 0.26°C (n = 5) higher than at the control site (n = 500, $\chi^2_{1,500}$ = 58602.48, p < 0.001) (Fig. 2a). SST decreases at rates of 0.003°C $m^{-1}$ (n = 500, $\chi^2_{1,500}$ = 8.86, p < 0.001) and 0.008°C $m^{-1}$ (n = 500, $\chi^2_{1,500}$ = 14.72, p < 0.001) on moving away from the discharge point at HZ in February and September respectively (Fig. 2a). This translates to a mean SST gradient of 0.006°C $m^{-1}$ and maximal SST difference of 0.6°C within a 100 m radius of the thermal effluent source. Seafloor temperature at the effluent source in June is elevated by 2.68 ± 0.64°C (n = 5) above control conditions (n = 510, $t_{509}$ = 9.24, p < 0.001) (Fig. 2a). On moving away from the effluent source, temperature within the *Posidonia oceanica* meadow declines at an exponential rate ($k$) of 0.05 $m^{-1}$ (n = 510, $t_{509}$ = 6.5, p < 0.001) (Fig. 2a), cor-

responding to a maximal temperature difference (ΔT) of 2.81°C within a 100 m radius of the outflow. Evidently this disparity between SST and temperature within the meadow is caused by a thermocline. The temperature gradient experienced by *P. oceanica* and its associated fauna is consequently much stronger than that observed at the sea surface. At the reference site, temperature does not change with distance in September (n = 500, $\chi^2_{1,500}$ = 1.35, p = 0.25) or June (n = 510, $t_{509}$ = 0.86, p = 0.39), but in February it increases at a minute rate of 0.0008°C $m^{-1}$ away from the shore (n = 500, $\chi^2_{1,500}$ = 28.25, p < 0.001) (Fig. 2a). Interactions between site and distance are also present in February (n = 500, $\chi^2_{1,500}$ = 13.24, p < 0.001) and September (n = 500, $\chi^2_{1,500}$ = 15.93, p < 0.001). The temperature gradient is therefore unique to HZ and provides a robust treatment for our natural experiment. Our effective natural temperature treatment corresponds to a ΔT of 0.39°C, derived from the exponential temperature decrease described by the equation $y = 2.83e^{-0.05x} + 23.85$ between $x$ = 36.35 m and $x$ = 68.63 m (cf. Section 2.2; sampling locations in Fig. 1 and data in Fig. 2a). This ΔT is equivalent to an SST increase expected due to climate change in the coming 2 decades for this region of the central Mediterranean (Assis et al. 2018) and is therefore conservative compared to end-of-century treatments and more relevant to near-future climate change.

In addition to this temperature dissimilarity, seawater is somewhat more acidic at HZ. At a mean pH of 7.77 ± 0.01 (n = 755) across months, the power station outlet has a $H^+$ concentration that is 1.51 times higher than at the reference site where the mean pH value is 8.09 ± 0.01 (n = 755) (Fig. 2b). This difference is maximal in February, when the $H^+$ concentration is 6.76 times higher at HZ (n = 500, $\chi^2_{1,500}$ = 3080.45, p < 0.001). These results indicate that the effluent has a pH that is consistently lower than reference seawater (Fig. 2b). Although a slight increase in pH away from the effluent source is visible across months (Fig. 2b), this was only statistically significant in February (n = 500, $\chi^2_{1,500}$ = 78.79, p < 0.001) and June (n = 510, $t_{509}$ = 11, p < 0.001). Additionally, there is no interaction between site and distance in February (n = 500, $\chi^2_{1,500}$ = 0.91, p = 0.34) or September (n = 500, $\chi^2_{1,500}$ = 0.97, p = 0.33). This is likely due to the higher variability in pH when compared to temperature (Fig. 2), which masks the within-site gradient and precludes reliable prediction by the distance explanatory variable. Salinity shows no within-site changes and is identical at both sites across months (36.96 ± 0.03‰, n = 753 for HZ, n = 755 for HK) and was thus deemed ecologically unimportant for our study.

### 3.2. *Posidonia oceanica*

Seagrass meadows are present from 10 and 20 m offshore at the reference site (HK) and at the site affected by the thermal effluent (HZ) respectively. At the plant level, the number of *P. oceanica* leaves $shoot^{-1}$ is 16.59% greater at HK than at HZ (n = 80, $F_{1,77}$ = 11.48, p = 0.001) but unaffected by distance from the effluent outlet (n = 80, $F_{1,76}$ = 1.13, p = 0.29) and from the shore at the control site (n = 80, $F_{1,76}$ = 2.55, p = 0.11) (Fig. 3a). There is no interaction between site and distance (n = 80, $F_{1,76}$ = 2.99, p = 0.09) and our first null hypothesis therefore cannot be rejected. In contrast, leaf area increases by 2.22 $cm^2$ $shoot^{-1}$ $m^{-1}$ away from the effluent source at HZ (n = 80, $F_{1,76}$ = 13.1, p < 0.001) with no such trend evident at HK (n = 80, $F_{1,76}$ = 0.12, p = 0.73) (Fig. 3b). Similarly, leaf (n = 80, $\chi^2_{1,80}$ = 10.57, p = 0.001) and epiphyte (n = 80, $\chi^2_{1,80}$ = 11.42, p < 0.001) biomass $shoot^{-1}$ increase at exponential rates ($k$) of 0.02 and 0.03 $m^{-1}$ away from the discharge point, with no distance effect present at HK (Fig. 3c,e). There are interactions between site and distance for leaf area (n = 80, $F_{1,76}$ = 8.59, p = 0.004), leaf biomass (n = 80, $\chi^2_{1,80}$ = 4.44, p = 0.04) and epiphyte biomass (n = 80, $\chi^2_{1,80}$ = 4.08, p = 0.04) so we can reject the corresponding null hypotheses and may attribute these changes to temperature. Neither leaf area (n = 80, $F_{1,76}$ = 1.72, p = 0.19) and biomass (n = 80, $\chi^2_{1,80}$ = 0.02, p = 0.88) nor epiphyte biomass (n = 80, $\chi^2_{1,80}$ = 0.03, p = 0.86) were different between the 2 sites at the model intercept. Interestingly, SLA, which is inversely related to tissue density, is 12.87% smaller at the effluent site (n = 78, $F_{1,75}$ = 26.19, p < 0.001) (Fig. 3d). Furthermore, SLA decreases away from the shore at a rate of 0.63 $cm^2$ $g^{-1}$ $m^{-1}$ at the control site (n = 78, $F_{1,74}$ = 23.66, p < 0.001) but remains unchanged at the effluent site (n = 78, $F_{1,74}$ = 2.28, p = 0.14) (Fig. 3d). However, since there is no interaction between site and distance (n = 78, $F_{1,74}$ = 1.6, p = 0.21), we cannot reject the null hypothesis that temperature has no effect on SLA.

Assessment of differentiation between leaf growth stages within each shoot provided a more detailed picture of plant-level temperature effects. For instance, the greater leaf number $shoot^{-1}$ at HK (Fig. 3a) is solely driven by juvenile leaves, which are 60.87% more abundant than at HZ (n = 240, $F_{1,234}$ = 25.21, p < 0.001) (Fig. S1 in the Supplement at www.int-res.com/articles/suppl/m707p015_supp.pdf). In contrast, the increase in leaf area $shoot^{-1}$ away from the effluent source (Fig. 3b) is influenced by adult (n = 240, $\chi^2_{1,240}$ = 5.04, p = 0.02) and intermediate (n = 240, $\chi^2_{1,240}$ = 12.55, p < 0.001) leaves, with respective $k$ val-

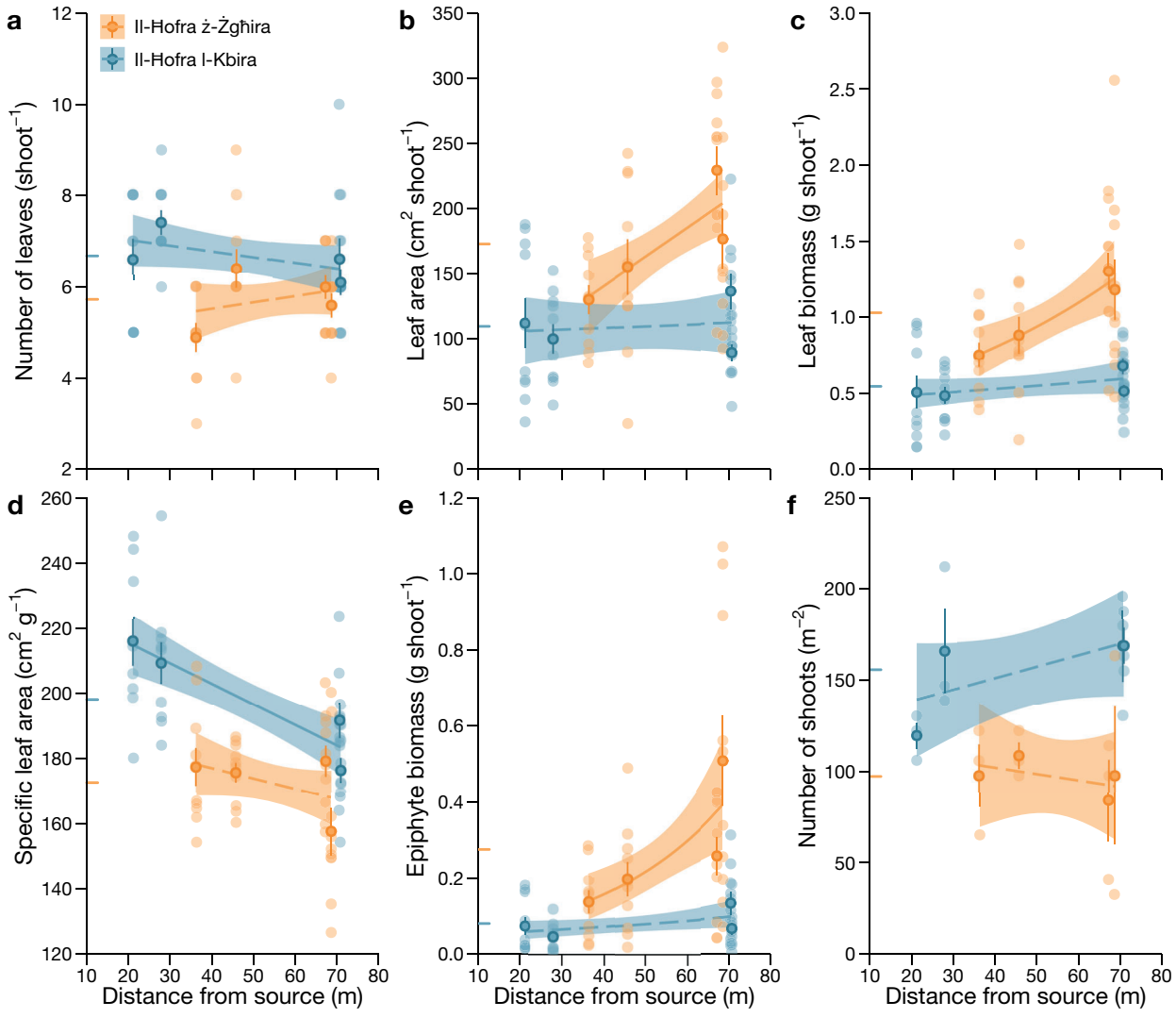


Fig. 3. *Posidonia oceanica* (a) leaf number, (b) leaf area, (c) leaf dry biomass, (d) specific leaf area, (e) epiphyte dry biomass and (f) shoot density in relation to distance from the effluent source (Il-Ħofra ż-Żgħira) and at the reference site (Il-Ħofra l-Kbira). Point-ranges are means ± SEM. Lines and ribbons are model predictions and 95% confidence intervals. Solid lines indicate significant change with distance at the 95% confidence level, while dashed lines indicate no change. Coloured *y*-axis ticks show overall means for each site

ues of 0.01 and 0.02 m$^{-1}$ (Fig. S2a). Similarly, the increase in leaf biomass shoot$^{-1}$ (Fig. 3c) is driven by adult (n = 240, $\chi^2_{1,240} = 5.78$, p = 0.02) and intermediate (n = 240, $\chi^2_{1,240} = 12.13$, p < 0.001) leaves, with *k* values of 0.01 and 0.02 m$^{-1}$ respectively (Fig. S2b). SLA clearly decreases as *P. oceanica* leaves grow (n = 237, $\chi^2_{2,237} = 182.56$, p < 0.001). Specifically, SLA is 48 and 143% higher in juvenile than in intermediate (n = 157, $t_{156} = 5.93$, p < 0.001) and adult (n = 158, $t_{157} = 13.69$, p < 0.001) leaves (Fig. S2c). This suggests that tissue density, toughness and longevity increase with leaf age. The decrease in SLA with increasing distance from the shore at HK (Fig. 3d) is only driven by adult leaves (n = 237, $\chi^2_{1,237} = 5.08$, p = 0.02) (Fig. S2c).

Seagrass shoot density is 60.14% higher at HK than at HZ (n = 24, $F_{1,21} = 18.26$, p < 0.001), while distance from the (hypothetical) effluent source has no effect at either HZ (n = 24, $F_{1,20} = 0.24$, p = 0.63) or HK (n = 24, $F_{1,20} = 2.18$, p = 0.16) (Fig. 3e). There is also no interaction between site and distance (n = 24, $F_{1,20} = 1.39$, p = 0.25) which indicates that the maximal ΔT of 0.39°C at HZ does not have a measurable effect on shoot density and we cannot reject the null hypothesis. However, shoot density is our seagrass variable with the lowest sample size (n = 24), so additional data may lead to a higher resolution and potential rejection of our null hypothesis. To test habitat-level effects of the thermal outflow, the 4

plant-level variables were multiplied by the mean shoot density at the respective plot. The resulting number of leaves $m^{-2}$ is 86.49% higher at HK than at HZ (n = 80, $\chi^2_{1,80}$ = 140.25, p < 0.001), but there is still no change along the temperature gradient (n = 80, $\chi^2_{1,80}$ = 0.28, p = 0.6) or interaction (n = 80, $\chi^2_{1,80}$ = 1.17, p = 0.28) (Fig. S3a). Leaf area $m^{-2}$ (n = 80, $F_{1,76}$ = 0.44, p = 0.51) (Fig. S3b), leaf biomass $m^{-2}$ (n = 80, $F_{1,76}$ = 0.77, p = 0.38) (Fig. S3c) and epiphyte biomass $m^{-2}$ (n = 80, $\chi^2_{1,80}$ = 1.7, p = 0.19) (Fig. S3d) do not display an interaction between site and distance and all increase on moving away from the shore at both sites. Therefore, the impact of the temperature gradient on *P. oceanica* is not appreciable at the habitat level, which may be due to differential thermal adaptation at different levels of the plant. Overall, surprisingly many attributes of *P. oceanica* are strongly affected by the relatively small but long-term *in situ* ΔT of 0.39°C.

### 3.3. Macrofauna

A total of 66 taxa of motile macrofauna across 5 (sub)phyla (Crustacea, Mollusca, Echinodermata, Annelida and Vertebrata) inhabit the *P. oceanica* meadows at HK and HZ. The most abundant and speciose taxa are Crustacea and Mollusca, with 35.06 ± 6.06 and 23.69 ± 4.46 ind. $net^{-1}$ and 7.44 ± 0.7 and 7.06 ± 0.73 species $net^{-1}$ (n = 16), respectively. The macrofaunal assemblage at HZ is markedly different from that at HK (n = 16, pseudo-$F_{1,14}$ = 8.86, p < 0.001) (Fig. 4), with the site difference explaining 38.76% of the variation in overall macrofaunal assemblage composition. Plots along the temperature gradient at HZ account for 59.15% of the within-site variance among the macrofaunal assemblage (n = 8, pseudo-$F_{3,4}$ = 1.93, p = 0.02), while the assemblage composition is similar between plots at HK (n = 8, pseudo-$F_{3,4}$ = 1.28, p = 0.26) (Fig. 4). Furthermore, plots A to D at HZ are visibly separated out along a gradient of increasing temperature in multidimensional space (see arrow in Fig. 4). This provides a first hint that macrofauna are affected by the *in situ* temperature elevation of 0.39°C at HZ, but univariate evidence is required to confirm the direction of this effect.

Macrofauna associated with *P. oceanica* meadows are 1.86 times more abundant at HZ than at HK (n = 16, $\chi^2_{1,16}$ = 34.61, p < 0.001), but there is no interaction (n = 16, $\chi^2_{1,16}$ = 0.22, p = 0.64) or change with distance from the thermal effluent source (n = 16, $\chi^2_{1,16}$ = 1.41, p = 0.23) (Fig. 5a). Species richness, on the other hand, decreases at a rate of 0.32 species $m^{-1}$ away from the thermal outflow (n = 16, $\chi^2_{1,16}$ = 29.15, p < 0.001), with no such change at the reference site (n = 16, $\chi^2_{1,16}$ = 1.21, p = 0.27) (Fig. 5b). Predicted species richness at HZ is higher than at the reference site within 82.81 m from the source (n = 16, $\chi^2_{1,16}$ = 23.4, p < 0.001). This increase in the number of species with rising temperature is mostly driven by Crustacea, as species richness for this subphylum follows a similar pattern, decreasing at a rate of 0.18 species $m^{-1}$ away from the discharge point (n = 16, $\chi^2_{1,16}$ = 13.21, p < 0.001), but with no change at the reference site (n = 16, $\chi^2_{1,16}$ = 0.28, p = 0.59). In contrast, Shannon-Wiener diversity is unaffected by site (n = 16, $\chi^2_{1,16}$ = 2.05, p = 0.15) and distance (n = 16, $\chi^2_{1,16}$ = 3.05, p = 0.08), while Pielou's evenness increases at a rate of 0.002 $m^{-1}$ away from the source (n = 16, $\chi^2_{1,16}$ = 11.82, p < 0.001) (Fig. 5c). Evenness does not change with distance at HK (n = 16, $\chi^2_{1,16}$ = 0.02, p = 0.89) and is therefore lower at HZ within 85.11 m from the discharge point (n = 16, $\chi^2_{1,16}$ = 9.3, p = 0.002). Hence, except for the case of macrofaunal abundance, we may reject our null hypotheses. While elevated temperature increases the number of species, it skews the assemblage towards few dominant species.

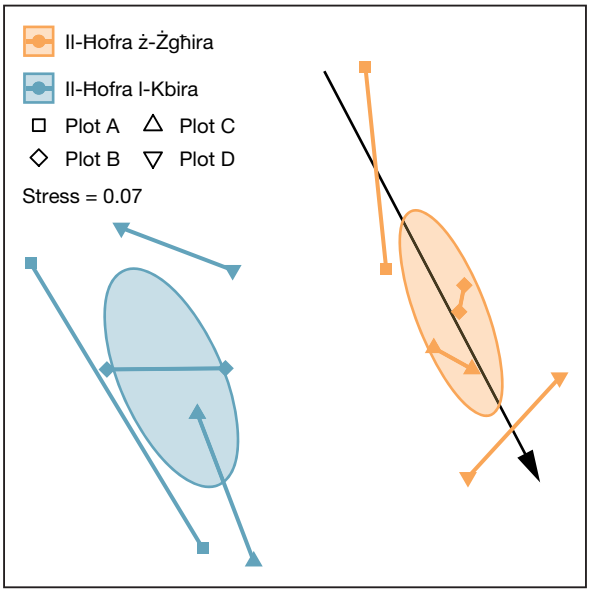


Fig. 4. Assemblage composition of motile macrofauna associated with *Posidonia oceanica* meadows at the site of thermal outflow (Il-Ħofra ż-Żgħira) and the reference site (Il-Ħofra l-Kbira). Each point represents one replicate. Lines connect replicates from the same plot. Ellipses are 95% confidence intervals around site centroids. The arrow indicates the approximate direction of temperature increase in multidimensional space. Plots A to D are located along the temperature gradient towards the effluent source, with A being the coolest and D the warmest plot (cf. Fig. 1)

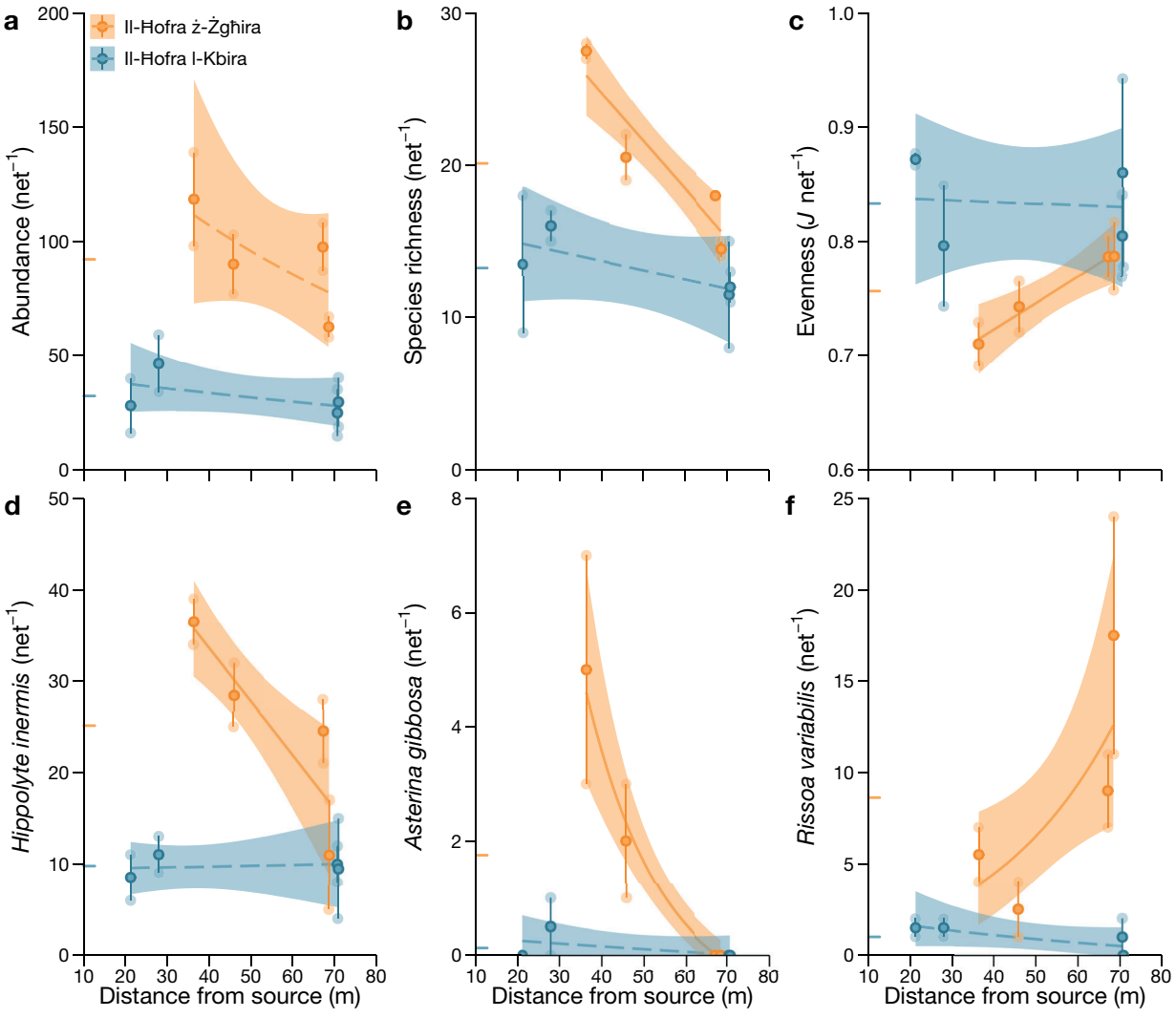


Fig. 5. Number of (a) macrofaunal individuals, (b) species and (c) Pielou's index of macrofaunal community evenness, along with (d–f) abundance of selected macrofaunal species associated with *Posidonia oceanica* in relation to distance from the effluent source (Il-Ħofra ż-Żgħira) and at the reference site (Il-Ħofra l-Kbira). Point-ranges are means ± SEM. Lines and ribbons are model predictions and 95% confidence intervals. Solid lines indicate significant change with distance at the 95% confidence level, while dashed lines indicate no change. Coloured *y*-axis ticks show overall means for each site

At the species-level, only 3 crustacean and 3 mollusc species account for 60.87% of the community variance between sites, all of which are more abundant at HZ (Table S1). Along the thermal gradient between plots A and D, 4 crustacean and 1 echinoderm species explain 46.87% of the within-site community variance, all of which are more abundant in plot D, the warmest sampling locality (Table S2; cf. Fig. 1). Of these species, the main driver of dissimilarity along the thermal gradient (23.07%) is the decapod *Hippolyte inermis* which is also the most abundant macrofaunal species across sites (17.44 ± 2.78 ind. net$^{-1}$). Its abundance decreases away from the effluent source at a rate of 0.59 ind. m$^{-1}$ (n = 16, $\chi^2_{1,16}$ = 13.15, p < 0.001), while there is no such change at the reference site (n = 16, $\chi^2_{1,16}$ = 0.03, p = 0.86) (Fig. 5d). Within 79.84 m of the discharge point, *H. inermis* is predicted to be more abundant than at the reference (n = 16, $\chi^2_{1,16}$ = 33.64, p < 0.001). Similarly, the abundance of echinoderm *Asterina gibbosa* decreases at $k$ = 0.06 m$^{-1}$ away from the source (n = 16, $\chi^2_{1,16}$ = 55.06, p < 0.001), but is unaffected at HK (n = 16, $\chi^2_{1,16}$ = 0.89, p = 0.35) (Fig. 5e). In contrast, the littorinid *Rissoa variabilis* increases at $k$ = 0.03 m$^{-1}$ away from the thermal outflow (n = 16, $\chi^2_{1,16}$ = 6.05, p = 0.01), with no trend at HK (n = 16, $\chi^2_{1,16}$ = 1.86, p = 0.17) (Fig. 5f). Interestingly, the abundance of the epiphyte grazer *R. variabilis* closely follows the increase

in epiphyte biomass shoot$^{-1}$ away from the effluent source, with an identical $k$ value of 0.03 m$^{-1}$ (cf. Figs. 3d & 5f). While unaffected by distance, mysids, the trochid *Jujubinus exasperatus* and the littorinid *Alvania discors* are 10 times (n = 16, $\chi^2_{1,16}$ = 53.21, p < 0.001), 6.6 times (n = 16, $\chi^2_{1,16}$ = 52.51, p < 0.001) and 3.1 times (n = 16, $\chi^2_{1,16}$ = 6.61, p = 0.01) more abundant at HZ, respectively.

## 4. DISCUSSION

The present study provides a first *in situ* assessment of the long-term effects of elevated seawater temperature on *Posidonia oceanica* and the motile macroinvertebrate assemblage associated with its meadows, a unique opportunity created by a thermal effluent that has been operating for 3 decades at HZ. Studies dealing with long-term effects of elevated sea temperature on *P. oceanica* meadows and associated biota within the natural setting of a coastal site appear to be unavailable. Therefore, the present results are deemed insightful. In turn, such insight may contribute to understanding and predicting the effects of sea warming on Mediterranean seagrasses and associated biota, which may then be used for conservation actions.

Other than temperature, only pH returned a statistically significant result with distance from the effluent source. However, regardless of statistical significance, the average pH gradient at HZ across months corresponds to 0.0009 m$^{-1}$, which is arguably not biologically relevant. Therefore, increasing distance from the effluent source cannot be used as a proxy for increasing pH and we excluded it as a potential factor influencing ecological within-site trends at HZ. Consequently, we specifically refer to distance from the effluent outlet as a temperature treatment while acknowledging that between-site differences are likely also influenced by pH and potential confounders.

Our results indicate the presence of a thermal gradient of around 0.006°C m$^{-1}$ at HZ, and an overall higher SST by 2.02 ± 0.54°C at the point of thermal outflow, when compared to an equivalent point at HK. When considering the temperature at the seafloor and therefore the temperature that is experienced by *P. oceanica* and the associated macrofauna, both the within-site temperature gradient, and the temperature difference between sites, are more pronounced at $k$ = 0.05 m$^{-1}$ and 2.68 ± 0.64°C respectively. The elevated sea temperature along such gradient would be expected to affect *P. oceanica* growing close to the thermal effluent discharge point. Sea temperature is arguably the most important range limiting factor for marine macrophytes, including seagrasses (Repolho et al. 2017). Within this context, several studies (Díaz-Almela et al. 2009, Marbà & Duarte 2010, Pagès et al. 2018) have reported adverse effects of elevated temperature on *P. oceanica*. Local studies undertaken as part of scientific projects at different times during the 3 decades when the thermal effluent was continuously present at HZ indicated persistent presence of healthy *P. oceanica* meadows. This observation is intriguing considering an expected decline of the seagrass resulting from the elevated sea temperature in the inlet. The present study again confirmed the presence of healthy *P. oceanica* meadows at HZ, but results indicate differences in shoot morphometric attributes when comparing data for the same seagrass from the nearby reference site HK.

Survival of *P. oceanica* under conditions of elevated sea temperature is supported by Ruocco et al. (2019), who show that *P. oceanica* possesses a degree of differential plasticity through epigenetic and gene expression processes that result in tolerance to heat stress. Immature leaves are energy sinks and depend on older more mature tissue to fuel growth. Downregulation of gene expression can arrest growth in the immature sections of the plant, allowing energy to be diverted to protective responses in the older sections of the plant. Despite these sections not being growth centres, without them there would be no energy acquisition to fuel growth (Ruocco et al. 2019). Essentially, the plant shifts its strategy from growth to protection to ensure long-term survival, which may explain the observed lower number of juvenile leaves recorded at HZ. Moving away from the thermal discharge outlet at HZ, *P. oceanica* shoot density and number of leaves per shoot remained unchanged but leaf area and biomass increased. The overall difference in shoot density values between HZ and HK is noteworthy, however this may result from confounders not considered in the present study which should be investigated in the future.

While adaptation of *P. oceanica* to elevated sea temperature may involve genetically controlled plasticity of tissue response, the seagrass may also be responding at the biochemical level by adjusting the fatty acid composition in its tissues. This strategy has been identified when exposing the seagrass to elevated water temperature in the laboratory. Populations of seagrass from different geographical regions living at different ambient seawater temperatures showed different levels of thermal tolerance: seagrass populations living in higher thermo-environments were more tolerant to heat stress (Beca-Carretero et

al. 2018). This tolerance is possible through changes in the fatty acid composition of the plant tissue, enabling physiological adaptation to heat stress. Such adaptation may explain the recorded long-term survival of *P. oceanica* at HZ, including of seagrass stands present in the vicinity of the thermal effluent discharge point at the inlet. *P. oceanica* ecotypes present at different water depths exhibit thermal adaptation, with meadows of the seagrass in shallow waters having the capacity to acclimate to heat stress via respiratory homeostasis and photo-protective mechanisms, providing further evidence of seagrass adaptation to elevated temperatures. Moreover, such mechanisms appear to be under genetic control (Marín-Guirao et al. 2017).

Although retention of the overall number of leaves per shoot may be an adaptive response to the elevated sea temperature at HZ, the decreased leaf area and biomass, together with the decrease in epiphyte abundance on moving towards the thermal discharge outlet, have an influence on seagrass habitat structure, which in turn affects the associated invertebrate assemblages (Boström & Bonsdorff 2000, Borg et al. 2010). On moving away from the thermal discharge outlet, macrofaunal species richness decreased but evenness increased. Such alteration in attributes of the biotic assemblages associated with the seagrass may be resulting from ecological factors that include altered habitat structure and food availability alongside effects of elevated temperature on physiological processes. Although the elevated sea temperature in the vicinity of the thermal effluent may be favouring some motile invertebrates, others such as the epiphyte grazer *Rissoa variabilis* showed decline which closely tracked the decrease in seagrass leaf epiphyte biomass. The trend for epiphyte biomass recorded in the present study corroborates previous findings, which indicated that seagrass leaf epiphytes decrease with an increase in water temperature (Hosokawa et al. 2009).

The decapod *Hippolyte inermis* is one of the most abundant species associated with the leaf stratum of *P. oceanica* habitat (Gambi et al. 1992, Borg & Schembri 2000), and contributed highly to the trends of species abundance and richness in this study. Despite the higher epiphyte biomass away from the effluent source, abundance of this shrimp decreases with distance from the thermal discharge outlet, whereas no such trend was recorded at HK. A possible, but untested explanation could be that *H. inermis* abundance is related to the abundance of the benthic diatom *Cocconeis neothumensis*, that grows epiphytically on *P. oceanica* leaves and is an important dietary component for the decapod's sex reversal strategy (Zupo 2000). Given that cell density and growth of *C. neothumensis* increase at elevated temperature (Ramírez et al. 2015), it is possible that, despite decreased macroepiphyte biomass, this microepiphyte provided *H. inermis* with more sustenance at higher temperatures. Alternatively, the thermal gradient in the vicinity of the thermal outfall may directly favour this crustacean's physiology (Zupo 1994). Assuming that there is a suitable level of food, thermal conditions may take precedence when determining an ideal environment for *H. inermis*, resulting in higher abundance of this species. One scenario does not necessarily exclude the other, and a combination of the proposed factors could be at play. There is a dearth of studies assessing the influence of elevated temperature on marine plant–animal interactions. However, one of them, which seems analogous to the outlined observation, found that increasing the water temperature increased the level of interaction between the alga *Sargassum filipendula* and the amphipod *Ampithoe longimana*, while temperature did not change the palatability of plant tissue to herbivores or the average herbivore feeding rate (O'Connor 2009). Another invertebrate whose abundance decreased away from the thermal effluent discharge point is the cushion sea star *Asterina gibbosa* but the underlying reason for this observation is unclear. Mysids, the trochid *Jujubinus exasperatus*, and the littorinid *Alvania discors* were also more abundant at the thermal effluent site (HZ) compared to the reference site (HK), although no change in their abundance with distance was evident. As in the case of *H. inermis*, the elevated sea temperature may be directly favouring their physiology, resulting in higher abundance. Increased sea temperature affects plant-herbivore interactions (Beca-Carretero et al. 2018), but the resulting effects are complex and not well understood (Hernán et al. 2017, Pagès et al. 2018).

In conclusion, the present results show that long-term elevated seawater temperature adversely impacts *P. oceanica* at the leaf level but does not necessarily lead to its demise at the plant level. The seagrass shows changes in morphometric features, possibly as a way to counteract thermal stress. Such morphometric changes, along with a decrease in leaf epiphyte biomass brought about by elevated seawater temperature, imply changes to seagrass habitat structure and availability of food, which influence the species composition and abundance of associated macrofauna. The direct effects of elevated temperature on physiological and other biological processes are also expected to lead to changes in the abun-

dance of macrofauna associated with the seagrass, thereby increasing the complexity of the ecosystem's response to warming. As a result, it is predicted that *P. oceanica* meadows in a warmer Mediterranean will experience a shift in plant morphology and associated macrofaunal community composition.

*Data availability*. All data and code from this study are available in the open-access repository maintained by L.S.W. (luka@wright.it) at https://github.com/lukaseamus/thermal-effluent. We place no restrictions on data and code availability within the constraints of the specified copyleft license.

*Acknowledgements*. The authors thank Maria Mangion for assistance with data processing, and Simon and Emma Gauci for providing the sampling vessel used during the survey. We are grateful to Julian Evans for assistance with identification of molluscs and echinoderms. This study was supported by funds granted to J.A.B. by the University of Malta.

*Author contributions*. J.A.B. and A.A. designed the study. A.A. collected all data. L.S.W. analysed and visualised all data and wrote the abstract, results and statistical methods. A.A. and J.A.B. wrote the introduction, methods and discussion. The manuscript was edited, revised and approved by all authors.

## LITERATURE CITED

Anderson MJ (2001) A new method for non-parametric multivariate analysis of variance. Austral Ecol 26:32–46

Anderson MJ (2006) Distance-based tests for homogeneity of multivariate dispersions. Biometrics 62:245–253

Assis J, Tyberghein L, Bosch S, Verbruggen H, Serrão EA, De Clerck O (2018) Bio-ORACLE v2.0: extending marine data layers for bioclimatic modelling. Glob Ecol Biogeogr 27:277–284

Beca-Carretero P, Guihéneuf F, Marín-Guirao L, Bernardeau-Esteller J, García-Muñoz R, Stengel DB, Ruiz JM (2018) Effects of an experimental heat wave on fatty acid composition in two Mediterranean seagrass species. Mar Pollut Bull 134:27–37

Bianchi CN, Morri C (2000) Marine biodiversity of the Mediterranean sea: Situation, problems and prospects for future research. Mar Pollut Bull 40:367–376

Borg JA, Schembri PJ (2000) Bathymetric distribution of decapods associated with a *Posidonia oceanica* meadow in Malta (Central Mediterranean). In: Von Vaupel Klein JC, Schram FR (eds) The biodiversity crisis and Crustacea. Crustacean Issue 12. AA Balkema, Rotterdam, p 119–130

Borg JA, Rowden AA, Attrill MJ, Schembri PJ, Jones MB (2010) Spatial variation in the composition of motile macroinvertebrate assemblages associated with two bed types of the seagrass *Posidonia oceanica*. Mar Ecol Prog Ser 406:91–104

Boström C, Bonsdorff E (2000) Zoobenthic community establishment and habitat complexity-the importance of seagrass shoot-density, morphology and physical disturbance for faunal recruitment. Mar Ecol Prog Ser 205:123–138

Boudouresque CF, Bernard G, Bonhomme P, Charbonnel E and others (2012) Protection and conservation of *Posidonia oceanica* meadows. RAMOGE and RAC/SPA, Tunis

Burgos E, Montefalcone M, Ferrari M, Paoli C, Vassallo P, Morri C, Bianchi CN (2017) Ecosystem functions and economic wealth: trajectories of change in seagrass meadows. J Clean Prod 168:1108–1119

Chefaoui RM, Duarte CM, Serrão EA (2018) Dramatic loss of seagrass habitat under projected climate change in the Mediterranean Sea. Glob Chang Biol 24:4919–4928

Clarke KR (1993) Non-parametric multivariate analyses of changes in community structure. Austral Ecol 18:117–143

de los Santos CB, Brun FG, Onoda Y, Cambridge ML, Bouma TJ, Vergara JJ, Pérez-Lloréns JL (2012) Leaf-fracture properties correlated with nutritional traits in nine Australian seagrass species: implications for susceptibility to herbivory. Mar Ecol Prog Ser 458:89–102

de los Santos CB, Onoda Y, Vergara JJ, Pérez-Lloréns JL and others (2016) A comprehensive analysis of mechanical and morphological traits in temperate and tropical seagrass species. Mar Ecol Prog Ser 551:81–94

Delignette-Muller ML, Dutang C (2015) fitdistrplus: an R package for fitting distributions. J Stat Softw 64(4):1–34

Díaz-Almela E, Marbà N, Martínez R, Santiago R, Duarte CM (2009) Seasonal dynamics of *Posidonia oceanica* in Magalluf Bay (Mallorca, Spain): Temperature effects on seagrass mortality. Limnol Oceanogr 54:2170–2182

EEC (1992) Council Directive 92/43/EEC on the conservation of natural habitats and of wild fauna and flora. Off J Eur Comm L 206:7–50

Fox J, Weisberg S (2019) An R companion to applied regression. SAGE Publications, Thousand Oaks, CAGambi MC, Lorenti M, Russo GF, Scipione MB, Zupo V (1992) Depth and seasonal distribution of some groups of the vagile fauna of the *Posidonia oceanica* leaf stratum: Structural and trophic analyses. PSZNI: Mar Ecol 13: 17–39

Gambi MC, Conti G, Bremec CS (1998) Polychaete distribution, diversity and seasonality related to seagrass cover in shallow soft bottoms of the Tyrrhenian Sea (Italy). Sci Mar 62:1–17

Giraud G (1979) Polugone de frequence de longuer des feuilles de *POSIDONIA OCEANICA* (Linnaeus) Delile. Rapp Comm IntExpl SciMer Mediter 25/26:25–217

González-Correa JM, Bayle Sempere JT, Sánchez-Jerez P, Valle C (2007) *Posidonia oceanica* meadows are not declining globally. Analysis of population dynamics in marine protected areas of the Mediterranean Sea. Mar Ecol Prog Ser 336:111–119

Guerrero-Meseguer L, Marín A, Sanz-Lázaro C (2017) Future heat waves due to climate change threaten the survival of *Posidonia oceanica* seedlings. Environ Pollut 230:40–45

Guerrero-Meseguer L, Marín A, Sanz-Lázaro C (2020) Heat wave intensity can vary the cumulative effects of multiple environmental stressors on *Posidonia oceanica* seedlings. Mar Environ Res 159:105001

Helber SB, Procaccini G, Belshe EF, Santillan-Sarmiento A and others (2021) Unusually warm summer temperatures exacerbate population and plant level response of *Posidonia oceanica* to anthropogenic nutrient stress. Front Plant Sci 12:662682

Hernán G, Ortega MJ, Gándara AM, Castejón I, Terrados J, Tomas F (2017) Future warmer seas: increased stress and susceptibility to grazing in seedlings of a marine habitat-forming species. Glob Chang Biol 23:4530–4543

Hosokawa S, Nakamura Y, Kuwae T (2009) Increasing temperature induces shorter leaf life span in an aquatic plant. Oikos 118:1158–1163

Huang P, Lin II, Chou C, Huang RH (2015) Change in ocean subsurface environment to suppress tropical cyclone intensification under global warming. Nat Commun 6: 7188

IPCC (2014) Climate Change 2014: Synthesis Report. Contribution of Working Groups I, II and III to the Fifth Assessment Report of the Intergovernmental Panel on Climate Change (Core Writing Team, Pachauri RK, Meyer LA [eds]). IPCC, Geneva

Jordà G, Marbà N, Duarte CM (2012) Mediterranean seagrass vulnerable to regional climate warming. Nat Clim Chang 2:821–824

Langford T (1990) Ecological effects of thermal discharges. Springer, Dordrecht

Lee KS, Park SR, Kim YK (2007) Effects of irradiance, temperature, and nutrients on growth dynamics of seagrasses: A review. J Exp Mar Biol Ecol 350:144–175

Marbà N, Duarte CM (2010) Mediterranean warming triggers seagrass (*Posidonia oceanica*) shoot mortality. Glob Change Biol 16:2366–2375

Marbà N, Duarte CM, Cebrián J, Gallegos ME, Olesen B, Sand-Jensen K (1996) Growth and population dynamics of *Posidonia oceanica* on the Spanish Mediterranean coast:elucidating seagrass decline. Mar Ecol Prog Ser 137:203–213

Marbà N, Duarte CM, Díaz-Almela E, Terrados J and others (2005) Direct evidence of imbalanced seagrass (*Posidonia oceanica*) shoot population dynamics in the Spanish Mediterranean. Estuaries 28:53–62

Marín-Guirao L, Ruiz JM, Dattolo E, Garcia-Munoz R, Procaccini G (2016) Physiological and molecular evidence of differential short-term heat tolerance in Mediterranean seagrasses. Sci Rep 6:28615

Marín-Guirao L, Entrambasaguas L, Dattolo E, Ruiz JM, Procaccini G (2017) Molecular mechanisms behind the physiological resistance to intense transient warming in an iconic marine plant. Front Plant Sci 8:1142

Marín-Guirao L, Bernardeau-Esteller J, García-Muñoz R, Ramos A and others (2018) Carbon economy of Mediterranean seagrasses in response to thermal stress. Mar Pollut Bull 135:617–629

Matteucci G, Magagnini M, Armeni M, Giaccaglia L and others (2011) Ecological assessment of a marine coastal area affected by a power plant water discharge (Brindisi, Adriatic Sea). Open Environ Biol Monit J 4:45–56

Mazzella L, Scipione MB, Buia MC (1989) Spatio-temporal distribution of algal and animal communities in a *Posidonia oceanica* meadow. PSZNI: Mar Ecol 10:107–129

O'Connor MI (2009) Warming strengthens an herbivore-plant interaction. Ecology 90:388–398

Oksanen J, Simpson GL, Blanchet FG, Kindt R and others (2020) vegan: community ecology package version 2.5-7. https://CRAN.R-project.org/package=vegan

Oksanen J, Blanchet GF, Friendly M, Kindt R and others (2014) veganCovEllipse. https://github.com/jarioksa/vegan/blob/master/R/veganCovEllipse.R (accessed 9 Feb 2020)

Ontoria Y, Cuesta-Gracia A, Ruiz JM, Romero J, Pérez M (2019) The negative effects of short-term extreme thermal events on the seagrass *Posidonia oceanica* are exacerbated by ammonium additions. PLOS ONE 14: e0222798

Orth RJ, Carruthers TJB, Dennison WC, Duarte CM and others (2006) A global crisis for seagrass ecosystems. BioScience 56:987–996

Pagès JF, Smith TM, Tomas F, Sanmartí N and others (2018) Contrasting effects of ocean warming on different components of plant–herbivore interactions. Mar Pollut Bull 134:55–65

Pielou EC (1966) The measurement of diversity in different types of biological collections. J Theor Biol 13:131–144

Pinheiro J, Bates D, DebRoy S, Sarkar D, R Core Team (2020) nlme: linear and nonlinear mixed effects models. R package v3.1-151. https://CRAN.R-project.org/package=nlme

R Core Team (2020) R: a language and environment for statistical computing. R Foundation for Statistical Computing, Vienna. https://www.r-project.org

Ramírez EE, González MA, Cifuentes AS, Inostroza I, Urrutia RE (2015) Culture and growth of two benthic diatoms species isolated from the Salar del Huasco (North of Chile, 20° S) at different conditions of temperature, light and nutrient. Gayana Bot 72:165–176

Repolho T, Duarte B, Dionísio G, Paula JR and others (2017) Seagrass ecophysiological performance under ocean warming and acidification. Sci Rep 7:41443

Revelle W (2020) Psych: procedures for psychological, psychometric, and personality research. R package v2.0.12. https://CRAN.R-project.org/package=psych

RStudio Team (2020) RStudio: integrated development environment for R. RStudio, Boston, MA

Ruiz JM, Marín-Guirao L, García-Muñoz R, Ramos-Segura A and others (2018) Experimental evidence of warming-induced flowering in the Mediterranean seagrass *Posidonia oceanica*. Mar Pollut Bull 134:49–54

Ruocco M, De Luca P, Marín-Guirao L, Procaccini G (2019) Differential leaf age-dependent thermal plasticity in the keystone seagrass *Posidonia oceanica*. Front Plant Sci 10: 1556

Russo GF, Fresi E, Vinci D (1985) The hand-towed net method for direct sampling in *Posidonia oceanica* beds. Rapp Comm Int Expl Sci Mer Mediter 29:175–177

Schiel DR, Steinbeck JR, Foster MS (2004) Ten years of induced ocean warming causes comprehensive changes in marine benthic communities. Ecology 85: 1833–1839

Shannon CE (1948) A mathematical theory of communication. Bell Syst Tech J 27:379–423

Telesca L, Belluscio A, Criscoli A, Ardizzone G and others (2015) Seagrass meadows (*Posidonia oceanica*) distribution and trajectories of change. Sci Rep 5:12505

Thomson JA, Burkholder DA, Heithaus MR, Fourqurean JW, Fraser MW, Statton J, Kendrick GA (2015) Extreme temperatures, foundation species, and abrupt ecosystem change: an example from an iconic seagrass ecosystem. Glob Chang Biol 21:1463–1474

Thorhaug A, Blake N, Schroeder PB (1978) The effect of heated effluents from power plants on seagrass (Thalassia) communities quantitatively comparing estuaries in the subtropics to the tropics. Mar Pollut Bull 9: 181–187

Waycott M, Duarte CM, Carruthers TJB, Orth RJ and others (2009) Accelerating loss of seagrasses across the globe threatens coastal ecosystems. Proc Natl Acad Sci USA 106:12377–12381

Wickham H (2016) ggplot2: elegant graphics for data analysis. Springer, New York, NY

Wilke CO (2020) cowplot: streamlined plot theme and plot annotations for 'ggplot2'. R package v1.1.1. https://CRAN.R-project.org/package=cowplot

Zupo V (1994) Strategies of sexual inversion in *Hippolyte inermis* Leach (Crustacea, Decapoda) from a Mediterranean seagrass meadow. J Exp Mar Biol Ecol 178:131–145

Zupo V (2000) Effect of microalgal food on the sex reversal of *Hippolyte inermis* (Crustacea: Decapoda). Mar Ecol Prog Ser 201:251–259

Zupo V, Buia MC, Mazzella L (1997) A production model for *Posidonia oceanica* based on temperature. Estuar Coast Shelf Sci 44:483–492

Zuur AF, Ieno EN, Walker N, Saveliev AA, Smith GM (2009) Mixed effects models and extensions in ecology with R. Springer, New York, NY

*Editorial responsibility: Morten Pedersen, Roskilde, Denmark*
*Reviewed by: X. Buñuel, J. R. Garcia-March and 1 anonymous referee*

*Submitted: December 26, 2021*
*Accepted: February 7, 2023*
*Proofs received from author(s): March 3, 2023*